Suppression of superconductivity in the $R(Ba_{1-z}R_z)_2Cu_3O_{7+\delta}$ (R=Pr,Nd) system

M. J. Kramer, K. W. Dennis, D. Falzgraf, and R. W. McCallum
Ames Laboratory, U.S. Department of Energy, Iowa State University, Ames, Iowa 50011

S. K. Malik
Tata Institute of Fundamental Research, Bombay 400005, India

W. B. Yelon
University of Missouri Research Reactor, Columbia, Missouri 65211

(Received 25 March 1997)

Structural and superconducting behavior of samples prepared with the nominal compositions of $Nd_{1.05}(Ba_{1-z}Pr_z)_{1.95}Cu_3O_{7+\delta}$ has been investigated by neutron-diffraction and dc magnetization measurements. Neutron data refined by the Reitveld method showed that there is mixing of the rare-earth (R) ions with a substantial fraction of the Pr going to the normal R site in the $RBa_2Cu_3O_{7+\delta}$-type structure and a corresponding fraction of the Nd going to the Ba site. Structural changes due to the trivalent R ions going to the Ba site are very similar to those observed in the $Nd_{1+x}Ba_{2-x}Cu_3O_{7+\delta}$ (Nd123ss), indicating that Pr behaves like other trivalent R's on the divalent Ba site. Magnetization measurements show that the depression in T_c is more pronounced for the Pr bearing samples than that for Nd123ss for the same number of trivalent ions on the Ba site. However, by correcting the changes in T_c for the depression associated with the fraction of Pr on the R site, the depression in T_c per trivalent ion on the divalent site is found to be identical to that in other light R123ss. Thus the depression in superconductivity in this series of samples is due to two independent effects: (1) Pr on the R site and (2) hole localization due to trivalent R ions on the Ba site. In this respect, Pr on the Ba site appears to behave like all the other trivalent R ions. [S0163-1829(97)03934-9]

I. INTRODUCTION

Unlike $YBa_2Cu_3O_{7-\delta}$ (Y123) which forms only as a stoichiometric compound, the light rare-earth elements (R) form a solid solution, with increasing substitution of the R^{3+} for the Ba^{2+} with increasing ionic radii of the R.[1,2] Additions of excess light rare-earth elements in $R_{1+z}Ba_{2-x}Cu_3O_{7+d}$ (R123ss) result in oxygen defects on the antichain sites.[3–5] In the $Nd_{1+x}Ba_{2-x}Cu_3O_{7+d}$ (Nd123ss) system, Nd^{3+} has an ionic radius approaching Ba^{2+}, allowing a high degree of solubility with Ba ($x \cong 0.8$) without forming second phases.[6] The superconducting properties of this system can be controlled via substitution of divalent Ba by trivalent Nd in addition to changing the oxygen stoichiometry. The depression in superconducting transition temperature (T_c) for fully oxygenated samples has been shown to be due to hole localization caused by filling the antichain site with oxygen in order to balance charges in the system.[7] In this case T_c depression is analogous to increasing δ in the stoichiometric R123 compounds. However, T_c can also be depressed by substituting Pr for R in the $R_{1-x}Pr_xBa_2Cu_3O_{7-\delta}$ (RPr123) systems.[8] In this case, the mechanism for depression is not well understood. While it has been suggested that the valence of the Pr ion is 4+ causing the number of conducting holes to decrease when tetravalent Pr ions are substituted on the trivalent rare-earth (R) sites,[9] considerable evidence indicates that Pr is trivalent in these materials.[10] Furthermore, electron-energy-loss spectroscopy measurements show that the total hole concentration in the (R,Pr)123 system does not change as the content of Pr increases.[11] It has also been suggested that strong hybridization of the Pr $4f$ states with O p orbitals destroys superconductivity.[12] This model, however, fails to explain the superconductivity which was found in thin-film $Pr_{0.5}Ca_{0.5}Ba_2Cu_3O_7$.[13]

In this study, we investigate the role of nominally substituting Pr onto the Ba sites in samples prepared with the nominal compositions of $Nd_{1.05}(Ba_{1-x}Pr_z)_{1.95}Cu_3O_{7+\delta}$. If Pr is a well behaved trivalent ion, and if all of the Pr remains on the Ba site, the suppression of T_c should be similar to that caused by Nd. Since Pr^{3+} is slightly larger than Nd^{3+} in size (1.013 Å vs 0.995 Å), there should be a preference for Pr to go to the Ba site compared to Nd based solely on lattice strain arguments. However, this preference is not large, so there is expected to be some site mixing of the two R's. If Pr tends toward the tetravalent state (0.90 Å), the Pr occupancy on the R site should be favored. For this reason, neutron-diffraction studies were performed to determine the relative site preferences of the Nd and Pr ions. dc magnetization measurements were performed to study the effect of Pr on the superconducting transition temperature.

II. EXPERIMENTAL TECHNIQUE

A. Sample preparation

Nd_2O_3 and $BaCO_3$ were dried at 1000 and 750 °C for 24 h, respectively. Pr_6O_{11} was dried at 900 °C for 24 h and at 400 °C for 24 h to insure the formation of stoichiometric Pr_6O_{11}. In order to fully oxidize CuO, it was dried at 550 °C for 5 days. Samples were made using conventional solid-state reactions. $Nd_{1.05}(Ba_{1-z}Pr_z)_{1.95}Cu_3O_{7+\delta}$ was

TABLE I. Rietveld refinements of the neutron-diffraction data for $R(Ba_{1-z},R_z)_2Cu_3O_{7+\delta}$. For $z<0.125$, the space group used is $Pmmm$ and $P4/mmm$ for $z\geqslant 0.125$. For the orthorhombic refinements, $R\frac{1}{2}\frac{1}{2}\frac{1}{2}$, $Ba\frac{1}{2}\frac{1}{2}z$, Cu_1000, Cu_200z, $O_10\frac{1}{2}0$, $O_2\frac{1}{2}0z$, $O_30\frac{1}{2}z$, O_400z, and $O_5\frac{1}{2}00$. For the tetragonal refinements O_1 and O_5 are equivalent and O_2 and O_3 are equivalent.

	$z=0.025$		$z=0.075$	$z=0.125$	$z=0.175$	$z=0.225$	$z=0.275$	$z=0.30$
a	3.853 73	(16)	3.859 96 (22)	3.884 74 (12)	3.882 92 (24)	3.881 32 (29)	3.877 18 (26)	3.883 24 (33)
b	3.909 13	(20)	3.900 32 (27)					
c	11.739 2	(6)	11.707 6 (9)	11.671 4 (5)	11.644 4 (8)	11.625 0 (9)	11.592 2 (1)	11.598 8 (13)
Vol.	176.848 1	(149)	176.259 (204)	176.135 8 (103)	175.563 1 (195)	175.126 1 (232)	174.260 4 (218)	174.904 0 (420)
Baz	0.183 3	(4)	0.182 5 (5)	0.1810 8 (31)	0.181 2 (4)	0.180 5 (4)	0.181 3 (5)	0.182 6 (6)
Cu_2z	0.349 34	(27)	0.3491 6 (3)	0.3499 8 (21)	0.3508 3 (29)	0.351 27 (30)	0.351 40 (40)	0.351 97 (44)
O_2z	0.370 95	(23)	0.3710 6 (26)	0.3711 1 (18)	0.3699 6 (25)	0.369 69 (26)	0.368 93 (29)	0.367 98 (36)
O_4z	0.157 87	(23)	0.1579 1 (26)	0.1581 4 (35)	0.1579 0 (47)	0.159 16 (57)	0.158 60 (66)	0.157 69 (79)
Nd (R)	1.000 0		0.971 (32)	0.927 (22)	0.839 (28)	0.761 (32)	0.733 (34)	0.728 (34)
Pr (R)			0.029 (32)	0.073 (22)	0.161 (28)	0.239 (32)	0.267 (34)	0.272 (34)
Nd (Ba)	0.250 0		0.04 (16)	0.062 (11)	0.106 (14)	0.144 (16)	0.158 (17)	0.136 (17)
Pr (Ba)			0.034 (16)	0.061 (11)	0.066 (14)	0.076 (16)	0.110 (17)	0.164 (17)
O_1 frac.	0.927	(19)	0.84 (24)	0.561 (10)	0.562 (12)	0.595 (14)	0.622 (15)	0.578 (15)
O_5 frac.	0.059	(15)	0.216 (21)					
O total	0.99		1.06	1.12	1.12	1.19	1.24	1.1562
χ^2	3.447		4.396	2.239	2.702	2.935	3.552	3.948
wR_p	0.0762		0.085 5	0.0607	0.0709	0.0735	0.0801	0.0833

prepared by mixing and heating appropriate amounts of Nd_2O_3, Pr_6O_{11}, $BaCO_3$, and CuO powders at 880 °C in air twice, then annealing at 940 °C in 100% O_2 three times with grinding in between. Oxygenation was performed on ground powders (<38 μm) at 450 °C for 24 h. Stoichiometric Nd123 was shown to be slightly overdoped with optimal doping occurring for 0.05 Nd on the Ba sites in the Nd123ss.[5] For this reason, all samples in this study were synthesized using 1.05 Nd atoms per formula unit. Heat treatments were repeated until x-ray-diffraction (XRD) and differential thermal analysis (DTA) confirmed the formation of a single-phase solid solution.

At this stage, the samples contained phase pure $(Nd,Pr)(Ba,Nd,Pr)_2Cu_3O_{7+\delta}$ solid solution. However, the degree of homogeneity of Nd or Pr throughout the entire sample is unknown since the driving force to form a solid solution is low. The only means of testing for short scale homogeneity (i.e., less than the coherence length) is to perform dc magnetization measurements and to look at both the magnitude of T_c as well as the sharpness of the superconducting transition. It was found that at least three anneals with intermediate grinding were necessary to insure homogeneity of the sample defined as a constant T_c and Meissner fraction between anneals.

B. Characterization

X-ray-diffraction (XRD) analysis was done by a Philips diffractometer equipped with a vertical 2-θ goniometer and Cu $K\alpha$ radiator. Typical scanning rates were 0.05° per step from 20° to 130°. Neutron-diffraction studies were performed at University of Missouri Research Reactor (MURR). Data were collected at room temperature on powders which were ground and sieved to a particle size of less than 25 μm. The neutron and XRD powder patterns were each refined by GSAS program software.[14] Differential thermal analysis was conducted with a Perkin-Elmer DTA 1700. The composition of the gases was controlled by a Sierra gas-flow controller. The gas-flow rate was 50 cc/min. The heating rate of the DTA furnace was set at 10 °C/min. The endothermic onset temperature was determined at the intersection point between the steepest tangent to the peak and the selected base line. A sample was not considered phase pure unless there were no discernible endothermic events before the peritectic decomposition (<2 wt. % CuO or $BaCuO_3$ phases present).

Magnetic and superconducting properties of the sample were studied by a Quantum Design MPMS superconducting quantum interference device magnetometer. Both field-cooled (FC) and zero-field-cooled (ZFC) magnetization data were obtained in 10 Oe applied field to determine T_c.

III. RESULTS AND DISCUSSION

A. Neutron diffraction

Table I presents the refined cell parameters for the $R(Ba_{1-z},R_z)_2Cu_3O_{7+\delta}$ series of samples where R can be either Nd or Pr. The Nd:Pr ratio is fixed by initial chemistry, but the site occupations for Nd and Pr on both the R and Ba sites were allowed to vary and were refined by Rietveld analysis of the neutron-diffraction data. In addition, the oxygen occupation for both O_1 (chain site) and O_5 (antichain site) were determined in the same way. In the case of $NdBa_2Cu_3O_{7-\delta}$, detailed analysis of Nd and Ba site occupancies showed that Ba does not go to the Nd site.[4] Similarly, analysis on the Nd excess Nd123ss samples showed that Ba does not go to the Nd site, while excess Nd goes to the Ba site.[7] Unfortunately, the neutron-scattering cross sections of Pr and Ba are very nearly the same and, therefore,

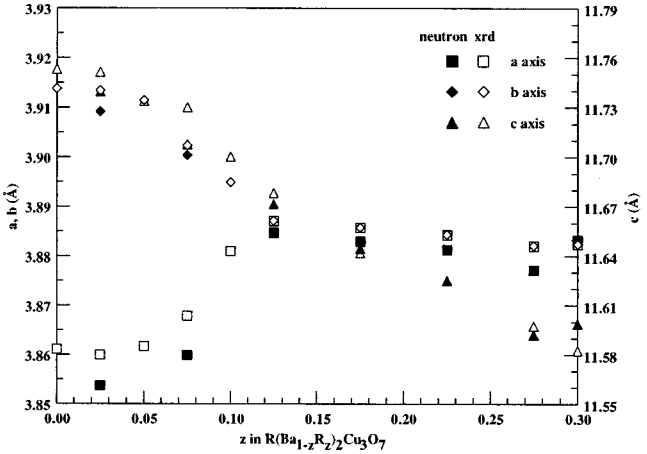

FIG. 1. Cell parameters for $R(Ba_{1-z}R_z)_2Cu_3O_{7+\delta}$ as a function of total R on the Ba site from neutron data in Table I (closed symbols) and XRD (open symbols).

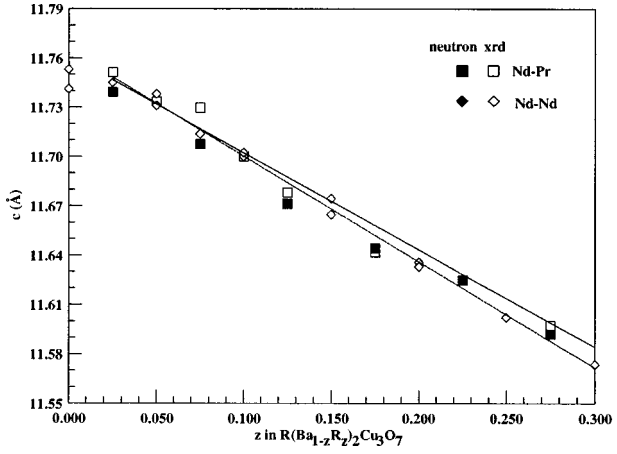

FIG. 2. Comparison of the contraction of the c axis with R on the Ba site for $R=$Nd alone and Nd-Pr. Closed symbols for neutron and open for XRD data.

these two cannot be distinguished uniquely. Therefore, in the subsequent analysis of site occupancies in the $Nd_{1.05}(Ba_{1-z}Pr_z)_{1.95}Cu_3O_{7+\delta}$ samples, it was assumed that the Ba fully occupies its normal site. After fixing the Ba occupancy, the Pr and Nd occupancies were allowed to vary freely both at the rare-earth site and at the nominal Ba site with the condition that combined fractional occupancies at the rare-earth site add up to unity (i.e., full occupancy) and likewise, the Ba, Pr, and Nd fractional occupancies at the nominal Ba site also add up to unity. This procedure was uniformly adopted for all the samples which gives a meaningful and reliable variation of Pr and Nd occupancies at the two sites.

For samples with $z<0.125$, the space group is $Pmmm$ (orthorhombic), while the structure collapsed to the tetragonal space group, $P4/mmm$, for higher substitutions of the trivalent rare earth for the divalent Ba ion. It should be recognized that O_1 and O_5 sites collapse to the O_1 site in tetragonal structure with a multiplicity of 2, while the O_2 and O_3 sites converge to the O_2. In Table I, the atomic site designations were not changed to reflect this increase in symmetry. In the Nd123ss, the loss of orthorhombicity was shown to be due to oxygen filling of the antichain sites to compensate additional charge arriving from the trivalent R substituting for the divalent Ba. The neutron-diffraction data confirm that this also occurs in the nominal Pr doping of the Ba site.

1. Structure

A composite plot of both neutron and XRD results shows that the c axis shortens with the increase in R on the Ba site (Fig. 1). This is consistent with the smaller R atom replacing the Ba atom. This change is nearly linear with z. Comparing the rate of change of the c axis with Nd on the Ba site for the Nd123ss, and that for the nominal Pr substitution on the Ba site, shows that there is little distinction between Nd and Pr substitution (Fig. 2). The average basal plane dimensions do not change with z for values less than 0.2. This would support the observation that the unit-cell volume change is primarily due to replacement of the larger Ba with the smaller R. The lack of clear distinction in the lattice contraction between nominal Pr on the Ba site and that of Nd on the Ba site supports the argument for the trivalent valence of the Pr since the difference in ionic radii between the Nd^{3+} and Pr^{3+} is $<2\%$.

Gross structural observations show little distinction between Nd and Pr, indicating that on the crystal structure level, there is little difference between Nd and Pr on the Ba site. Yet, as will be discussed later, the Pr bearing samples behave quite differently magnetically and electronically. For this reason, we must delve deeper to look for structural anomalies.

Figure 3 shows that the ratio of Nd:Pr on the R site changes with increasing Pr. Again, note that the samples, purposefully synthesized with slight excess Nd. This was done since the stoichiometric Nd123 is not stable at high

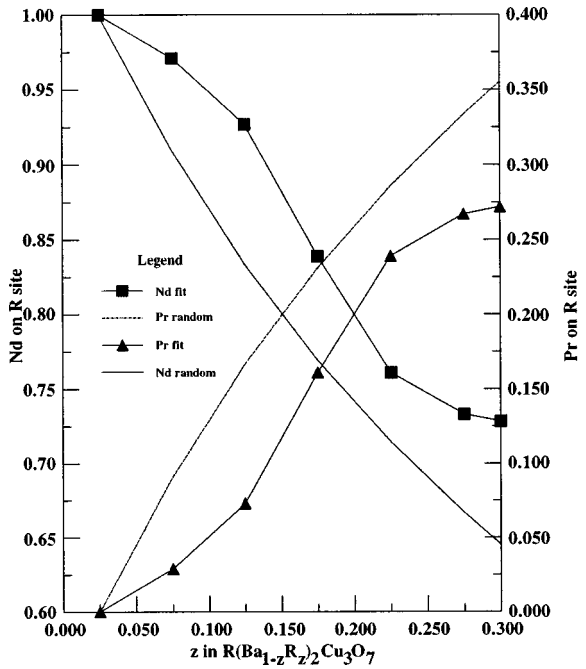

FIG. 3. Comparison of the Nd and Pr occupations on the R site for random mixing and that determined by Rietveld refinement of the neutron data.

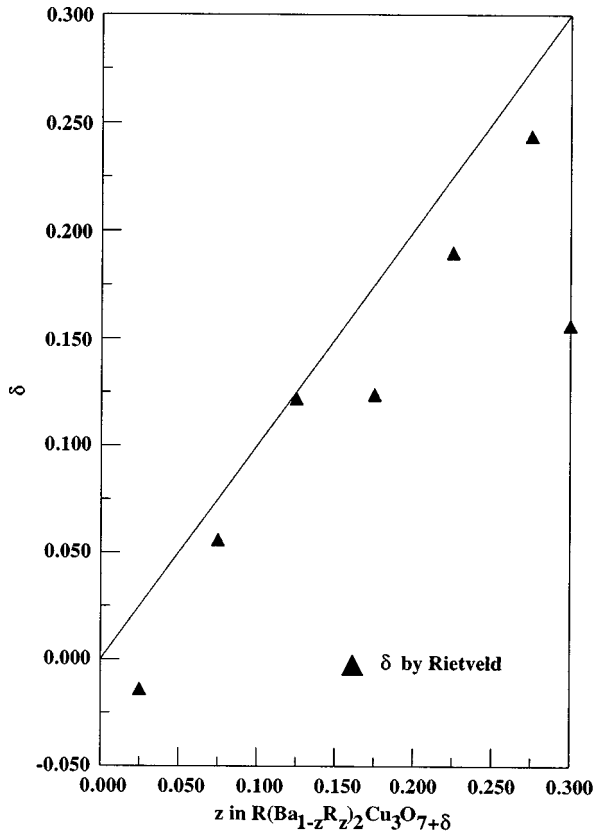

FIG. 4. Excess oxygen over 7 determined from neutron data.

temperatures with 1 bar PO_2 necessary to insure homogeneous single-phase samples. In addition, optimal doping for fully oxygenated Nd123ss occurs for excess Nd ($x \sim 0.05$). The solid lines represent the random mixture of Nd and Pr at the R and Ba site. The neutron data show that the Nd prefers the R site over Pr compared to random mixing. Based on ionic size arguments alone, this is expected since the Nd is slightly smaller.

2. Oxygen content

Rietveld refinement of the chain and antichain site oxygen occupancies indicates that the charge compensation is deficient in most samples (Fig. 4), even though a prolonged low-temperature (450 °C) oxygenation was performed on ground powders. This suggests that the distribution of trivalent ions on divalent sites is not random. Since only $\frac{1}{2}$ of an oxygen is needed to balance charge of the trivalent ion on the Ba site, the distribution or the R on the Ba sites determines how much excess oxygen a sample can uptake. It was observed that, in the Nd123ss, for doping levels of $0.1 < x < 0.4$, the T_c could be varied considerably depending on how the samples were processed.[3] Higher T_c's were observed for samples annealed at high temperatures in 1% PO_2. It was postulated that the lower oxygen partial pressure enhances the pairing of trivalent ions across antichain sites. Pairing would reduce the number of excess holes due to partially compensated oxygen on antichain sites and reduce hole localization due to hole robing by uncompensated trivalent ions on the Ba sites. The lack of complete charge compensation in the bulk suggests poor pairing of the trivalent ions

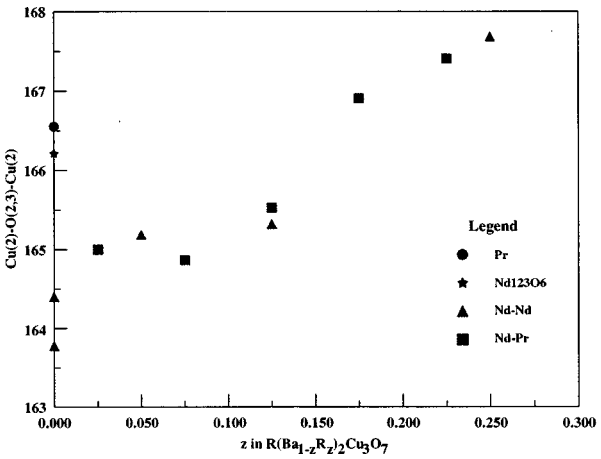

FIG. 5. Buckling of the Cu-O plane (angle between Cu_2-O_2, O_3-Cu_2) for $R(Ba_{1-z}R_z)_2Cu_3O_{7+\delta}$ for R=Nd or Pr alone and Nd-Pr.

on the Ba sites. This, however, is consistent with results from the Nd123ss samples prepared in a similar manner.[3]

3. Buckling of the Cu-O plane

Guillaume *et al.*[15] showed that the presence or absence of superconductivity in $R123$ compounds correlated strongly with the buckling of the Cu-O planes (critical angle of 167.3°). In the comparison between fully oxygenated Pr123 and the other superconducting $R123$ stoichiometric compounds, it was shown that the contraction in the c axis is due

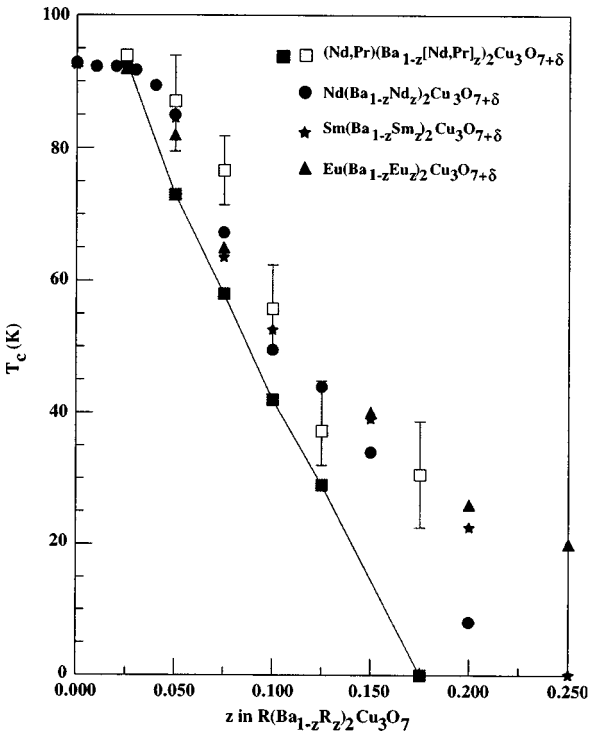

FIG. 6. T_c (taken at 90% of the ZFC diamagnetic signal 10 K for an applied field of 10 Oe) vs z in $R(Ba_{1-z}R_z)_2Cu_3O_{7+\delta}$ for a wide range of light R's on the Ba site. The Pr bearing samples contain Pr on the R and on the Ba site as shown in Table I. The open squares are for T_c when corrected for the depression due to Pr on the R site.

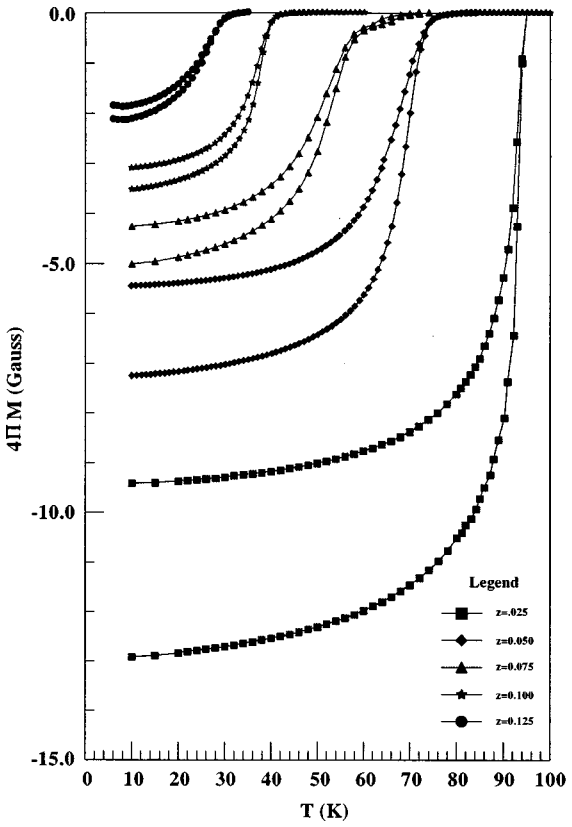

FIG. 7. Field-cooled (FC) and zero-field-cooled (ZFC) magnetization measurements with an applied field of 10 Oe for the $(Nd,Pr)(Ba_{1-z}[Nd,Pr]_z)_2Cu_3O_{7+\delta}$ samples. The Meissner fraction and T_c decrease with increasing z.

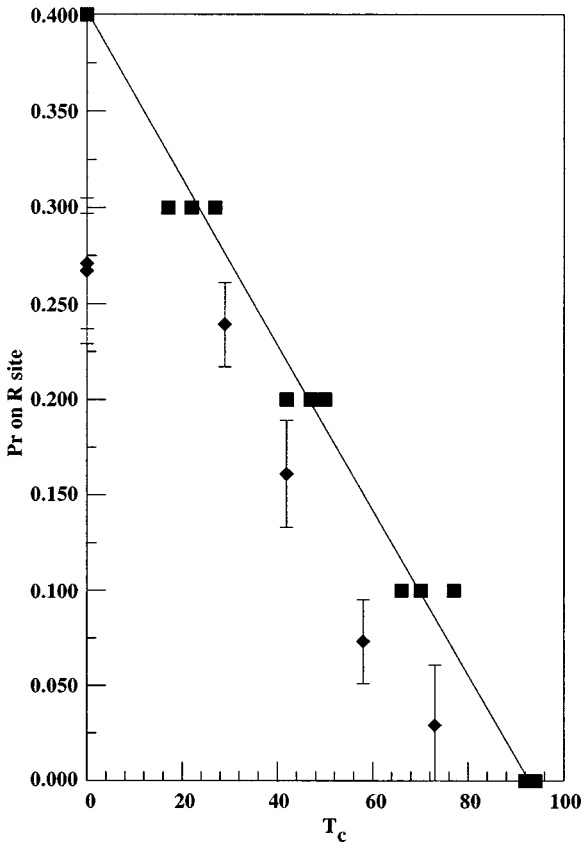

FIG. 8. T_c vs Pr occupation on the R site. The scatter in the T_c for the $(Nd,Pr)Ba_2Cu_3O_{7+\delta}$ samples (closed square symbol) is due to processing induced variations. The fitted line is only to that set of samples processed most like the $(Nd,Pr)(Ba[Nd,Pr])_2Cu_3O_{7+\delta}$ samples. The error bars on the $(Nd,Pr)(Ba[Nd,Pr])_2Cu_3O_{7+\delta}$ samples (closed diamonds) is the first σ of the fitted neutron data. The difference in T_c of the $(Nd,Pr)(Ba[Nd,Pr])_2Cu_3O_{7+\delta}$ samples from the fitted line is assumed to be due to hole localization from R on the Ba site.

to an increase in the puckering of the Cu-O planes resulting in a decrease in the Pr-O_2/O_3 distances.[15] In oxygen-deficient samples ($\delta \sim 1$), the puckering was similar for all $R123$ compounds, including Pr123. Figure 5 shows that the buckling of the Cu-O planes increases both with Nd and Pr going to the Ba site and that this puckering is similar to that seen in oxygen-deficient samples. There is a strong correlation between the degree of puckering and loss of T_c, so whatever is causing the Cu-O planes to distort from the ideal configuration also appears to be affecting superconductivity. In addition, this puckering occurs with either the removal of oxygen from the chain sites or filling of the antichain oxygen sites, reiterating the structural similarities between removal of oxygen in stoichiometric $R123$ and substitution of the trivalent R for Ba.

B. Magnetization measurements

The structural similarities between the oxygen-deficient $R123$ and the excess $R123$ss extend to their electronic structure.[7] Not only does T_c drop with increasing δ in $R123$ and with increase in x in $R_{1+x}Ba_{2-x}Cu_3O_{7+\delta}$, the details of the suppression are also similar. This includes the plateau with a T_c near 90 K for low doping levels and a second plateau with a T_c near 50 K for intermediate doping levels where the orthorhombic/tetragonal transition occurs. However, this analog breaks down for the Pr-doped samples studied here. Figure 6 shows that, for a range of $R123$ss samples (R is Nd, Sm, and Eu), T_c is nearly identical over a wide range of doping levels, diverging only at higher doping levels for reasons not fully understood. The Pr-doped samples, however, show a more precipitous and linear drop in T_c with Pr content. In addition to the drop in T_c, there is also a decrease in the Meissner fraction with increasing Pr content (Fig. 7). The drop in the Meissner fraction would suggest that a second, nonsuperconducting phase is forming. However, this is not borne out by the structural and DTA analysis.

It is well known that Pr on the R site in RPr123 compounds does suppress superconductivity. The neutron-diffraction analysis shows that a substantial fraction of the Pr is going to the R site in the compounds under investigation. If it is assumed that the depression in superconductivity in these samples is due to two independent effects, (1) Pr on the R site for whatever reason and (2) R on the Ba site resulting in hole localization, it should be possible to separate out these two effects if they can be measured independently. Figure 6 shows that for $z < 0.2$, the depression in T_c is independent of R except for Pr-doped samples. On the other hand, structurally Pr on the Ba site appears to behave as any other R. If it is assumed that the enhanced suppression in T_c is solely due to the Pr on the R site, and we have accu-

rately measured Pr occupancy on the R site, we need to only determine the functional dependence of T_c Pr (R site) to determine if Pr on the Ba site has any effect on T_c.

1. Effect of T_c for Pr on R site

Figure 8 shows the suppression of T_c due to Pr on the R site in $Nd_{1.05-y}Pr_yBa_{1.95}Cu_3O_7$. Again, a slight excess of Nd on the Ba site was used to obtain optimal doping level for superconductivity. For the optimally doped samples, Pr depresses superconductivity in a systematic, linear fashion. There is some variance in T_c depending on how the samples are prepared.[16] The T_c's for $Nd_{1.05}(Ba_{1-z}Pr_z)_{1.95}Cu_3O_{7+\delta}$ is plotted against the measured site occupancy of Pr on the R site from Table I and compared to the T_c's for $Nd_{1.05-y}Ba_{1.95}Cu_3O_7$ and its known site occupancies. Any deviation in T_c from the ideal case of Pr alone on the R site must then be due to hole localization by the trivalent ions on the Ba site. Correcting the T_c's shown in Fig. 6 for the effect of Pr on the R site (Fig. 8) shows that the corrected T_c's for the $Nd_{1.05}(Ba_{1-z}Pr_z)_{1.95}Cu_3O_{7+\delta}$ samples follow the same curve as the other R123ss. This indicates, that at least to the first order, the suppression in superconductivity in the $Nd_{1.05}(Ba_{1-z}Pr_z)_{1.95}Cu_3O_{7+\delta}$ system is due to two independent effects, one due to Pr on the R site and the other hole localization due to the effect of the trivalent ion on the divalent site. Recent work on the $Eu(Ba_{1-z}Pr_z)_2Cu_3O_{7+\delta}$ system, where there is a larger difference in ionic radii between Eu and Pr, indicates that Pr shows a strong affinity to substitute at the larger Ba site and a much reduced depression in T_c compared to that in the $Nd_{1.05}(Ba_{1-z}Pr_z)_{7+\delta}$ set of samples.[17]

IV. CONCLUSIONS

In this study, we have investigated the role of nominally substituting Pr onto the Ba sites in samples prepared with the nominal compositions of $Nd_{1.05}(Ba_{1-z}Pr_z)_{1.95}Cu_3O_{7+\delta}$. Neutron-diffraction data refined by the Rietveld method show that there is mixing of the R ions with a substantial fraction of the Pr going to the normal R site and some Nd going to the Ba site. Structural changes due to the trivalent R ions going to the Ba site are very similar to the Nd123ss, indicating that Pr behaves like other R on the Ba site. Magnetization measurements show that the depression in T_c is more pronounced for the Pr bearing samples. However, on correcting the changes in T_c for the fraction of Pr on the R site, this system also shows identical depression in T_c as with other light R123ss. Thus the depression in superconductivity in this set of samples is due to two independent effects: (1) Pr on the R site and (2) hole localization due to trivalent ions on the Ba site; Pr on the Ba site appears to behave like all the other trivalent R ions.

ACKNOWLEDGMENTS

This work was performed at Ames Laboratory, and was supported by the Director of Energy Research, U.S. Department of Energy under Contract No. W-7405-ENG-82. The work at MURR was supported by the U.S. Department of Energy Grant No. DE-FE02-90ER45427 through the Midwest Superconductivity Consortium.

[1] P. Karen, O. Braaten, and A. Kjekshus, Acta Chem. Scand. **52**, 805 (1992).
[2] K. Osamura and W. Zhang, Z. Metallkd. **84**, 522 (1993).
[3] R. W. McCallum, M. J. Kramer, K. W. Dennis, M. Park, H. Wu, and R. Hofer, J. Electron. Mater. **24**, 1931 (1995).
[4] K. Takita, H. Akinaga, T. Ohshima, Y. Takeda, and M. Takano, Physica C **191**, 509 (1992).
[5] S. I. Yoo and R. W. McCallum, Physica C **210**, 157 (1993).
[6] Y. Matsui, S. Takekawa, and N. Iyi, Jpn. J. Appl. Phys. **26**, L1693 (1987).
[7] M. J. Kramer, S. I. Yoo, R. W. McCallum, W. B. Yelon, H. Xie, and P. Allenspach, Physica C **219**, 145 (1994).
[8] For reviews see H. B. Radousky, J. Mater. Res. **7**, 1917 (1992); S. K. Malik and C. V. Tomy, in *Physical and Material Properties of High-T_c Superconductors*, edited by S. K. Malik and S. S. Shah (Nova Science, New York, 1994), p. 283.
[9] M. Andersson, Ö. Rapp, and R. Tellgren, Physica C **205**, 105 (1993).
[10] L. Soderholm, C. K. Loong, G. L. Goodman, and B. D. Dabrowski, Phys. Rev. B **43**, 7923 (1991).
[11] J. Fink, N. Nuecker, H. Romberg, M. Alexander, M. B. Maple, J. J. Neumeier, and J. W. Allen, Phys. Rev. B **42**, 4823 (1990).
[12] Y. Takano, S. Yokoyama, K. Kanno, and K. Sekizawa, Physica C **252**, 61 (1995).
[13] D. P. Norton, D. H. Lowndes, B. C. Sales, J. D. Budai, B. C. Chakoumakos, and H. R. Kerchner, Phys. Rev. Lett. **66**, 1537 (1991).
[14] Larson & Von Dreele, GSAS program software, 1988.
[15] M. Guillaume, P. Allenspach, W. Henggeler, J. Mesot, B. Roessli, U. Staub, P. Fisher, A. Furrer, and V. Trounov, J. Phys.: Condens. Matter **6**, 7963 (1994).
[16] A. Das, R. Suryanarayanan, I. Zelenay, and B. Babrowski, Physica C **273**, 301 (1997).
[17] Y. Xu, A. O'Connor, S. Malik, H. Wu, M. J. Kramer, and R. W. McCallum (unpublished).